Electronic Supplementary Material (ESI) for Environmental Science: Nano.

Emerging investigator series: Differential effects of carbon nanotube and graphene on the tomato rhizosphere microbiome

Yaqi You,[1,2,†] Patricia Kerner,[2] Sudha Shanmugam,[3] Mariya V. Khodakovskaya[3]

[1]Department of Environmental Resources Engineering, SUNY College of Environmental Science and Forestry, Syracuse, NY, USA

[2]Department of Biological Sciences, Idaho State University, Pocatello, ID, USA

[3]Department of Biology, University of Arkansas at Little Rock, Little Rock, AR, USA

[†]Correspondence:

Yaqi You

402 Baker Lab, 1 Forestry Dr, Syracuse, NY 13210

Email: yyou@esf.edu

Phone: +1-315-470-6765

Number of Pages: 25

Number of Figures: 9

Number of Tables: 4

Materials and Methods

Soil physicochemical property analyses

Tomato plants were grown in soils receiving either carbon nanotube (CNT) or graphene treatment, with appropriate controls included in each exposure experiment (6 biological replicates x 2 carbon nanomaterials (graphene or CNT) x 2 conditions (treatment or control) = 24 pots in total). After the exposure experiment, tomato plants were carefully removed. Bulk soil was mixed within each of the experimental pots.

For each carbon nanomaterial (CNM) and experimental condition, bulk soils from three replicate pots were mixed in equal amounts and analyzed for soil properties at the Environmental Analytical Laboratory, Brigham Young University (Provo, UT) using established protocols (https://pws.byu.edu/eal). Briefly, pH and electrical conductivity (EC) were measured using meters on a saturated soil paste. Ammonium (NH_4-N) and nitrate (NO_3-N) were extracted with 2 M potassium chloride (KCl) and measured on a Rapid Flow Analyzer (Quick Chem 8500, Lachat Instruments, Loveland, Colorado, USA). Cation exchange capacity (CEC) was measured with the ammonium replacement method on the same instrument. Organic matter (OM; in %) was measured by dichromate oxidation. Total C (%) and N (%) were determined based on combustion on an element analyzer (TruSpec CN Determinator, LECO Instruments, MI, USA). Phosphorus (P) was extracted with 0.5 M sodium bicarbonate ($NaHCO_3$) according to Olsen's method.[1] Exchangeable potassium (K) was extracted with ammonium acetate, sulfate (SO_4-S) was extracted with monocalcium phosphate, and micronutrients zinc (Zn), iron (Fe), manganese (Mn) and copper (Cu) were extracted with diethylenetriamine pentaacetate (DTPA). The extracted analytes were measured by inductively coupled plasma optical emission spectrometry (ICP-OES) (iCAP 7400, Thermo Electron, WI, USA). Calcium carbonate ($CaCO_3$) was measured according to Allison et al. (1965).[2] We chose extraction methods over total digestion methods in order to focus on bioavailable chemicals.

Soil basal respiration assessment

To evaluate CNM effects on the functionality of the soil microbial community, we first performed EcoPlate assay to compare substrate utilization patterns in bulk soils harvested at the conclusion of the exposure experiment (detailed in the main text). Next we used a microcosm setup to measure soil basal respiration (Figure S1). Bulk soil collected from a pot was thoroughly mixed and 10 grams were transferred to a sterile 50 mL amber serum bottle. The water content was maintained at 11% (w/w), a typical field capacity, using sterile Milli-Q water. Each serum bottle was sealed with a rubber septum and aluminum crimp, and incubated

for 1 hour in a growth chamber (model A1000, Conviron, Winnipeg, Canada) at 25 °C and under 50% humidity. Gas accumulated in bottle headspace was sampled using a 30 mL polypropylene syringe and immediately injected into an EGM-4 gas analyzer (PP systems, Amesbury, MA) for CO_2 measurement. Ambient CO_2 level was measured before each sampling to ensure analytical consistency.

Figure S1. Serum bottle microcosm for bulk soil respiration potential assessment. Bottles were incubated for 1 hour in a controlled growth chamber.

Results and Discussion

Changes in soil property due to carbonaceous nanomaterials (CNMs)

It should be noted that the CNT and graphene experiments were conducted using two different soils. Comparisons between bulk soils harvested from the control and treatment pots showed CNT and graphene treatment resulted in differential changes in soil property (Table S1).

Table S1. Properties of bulk soils from the control and treatment pots. After the removal of plant, bulk soil was mixed in the original pot and representative bulk soils from three replicate pots under each condition were mixed and analyzed for extractable chemicals. Relative changes higher than 50% were highlighted in bold.

	CNT.control	CNT	Relative change	Graphene.control	Graphene	Relative change
pH	6.66	6.54	-1.8%	6.09	6.06	-0.5%
EC (dS/m)	0.4	0.7	**73.8%**	0.7	0.8	15.4%
CEC (meq/100g)	67.3	56.1	-16.7%	66.1	75.7	14.5%
OM (%)	32.2	31.8	-1.1%	34.2	44.3	29.6%
Total C (%)	15.3	16.2	6.3%	14.3	18.1	26.5%
Total N (%)	0.420	0.444	5.7%	0.460	0.490	5.4%
NO_3-N (ppm)	9.0	10.9	21.4%	2.74	3.17	15.7%
NH_4-N (ppm)	8.1	7.9	-2.6%	22.3	26.0	16.5%
C:N	36.4	36.6	0.5%	31.0	37.1	20.0%
P (ppm)	34.6	34.0	-1.5%	33.2	20.9	-37.2%
K-av (ppm)	655	570	-12.9%	391	342	-12.7%
SO_4-S (ppm)	20.3	71.2	**250.1%**	589	593	0.7%
$CaCO_3$ (%)	7.20	2.98	**-58.6%**	0.99	1.50	**52.1%**
Zn (ppm)	0.17	0.22	25.8%	5.96	5.70	-4.4%
Fe (ppm)	27.90	13.99	**-49.9%**	149	142	-4.4%
Mn (ppm)	1.96	1.33	-32.0%	3723	3559	-4.4%
Cn (ppm)	0.26	0.33	27.2%	93086	88984	-4.4%

CNT affected more taxa of tomato-associated soil microbiomes

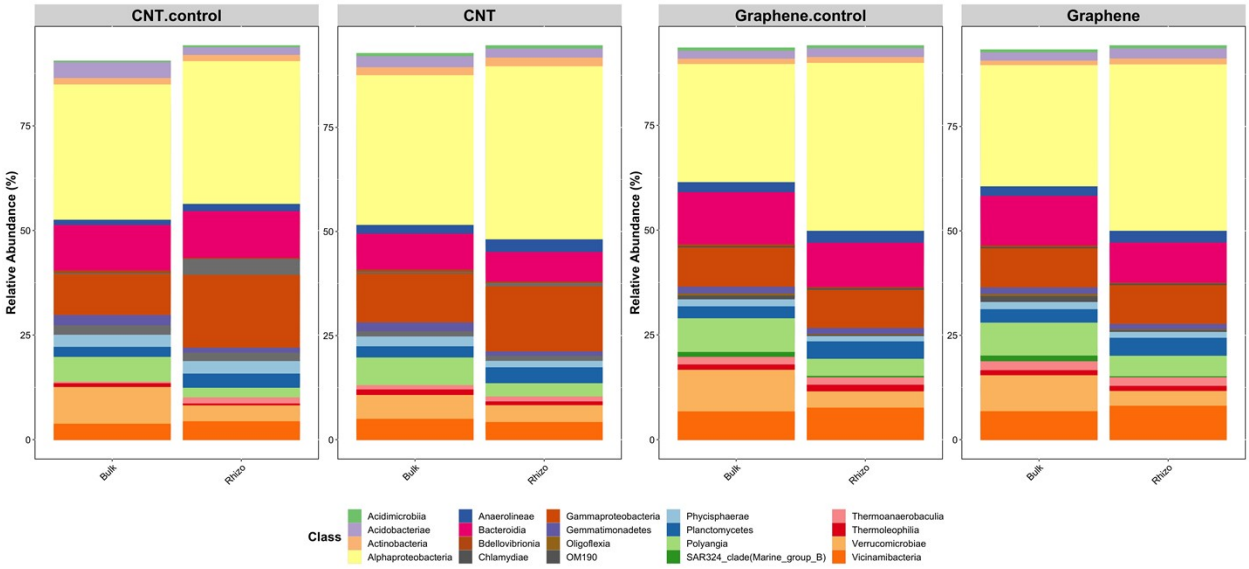

Figure S2. Effects of CNT (left) and graphene (right) on the relative abundance of the top 20 classes in the bulk soil and the tomato rhizosphere. Data were averaged among the biological replicates in each experiment.

Table S2. LEfSe identified differential taxa at the phylum or class level that were most likely to explain CNM-induced microbiome shifts. Asterisks indicate differential taxa common in bulk soil and the rhizosphere in either the CNT or graphene experiment. Taxa seen under both CNT and graphene treatment are in bold.

Treatment	Soil zone	Enriched		Suppressed	
		phylum	class (phylum in parentheses)	phylum	class (phylum in parentheses)
CNT	Bulk soil	Latescibacterota	*Blastocatellia (Acidobacteriota)	*BD2-11 terrestrial group	Bathyarchaeia (Crenarchaeota)
		*WS2	Subgroup 5 (Acidobacteriota)		Acidobacteriae (Acidobacteriota)
			Vicinamibacteria (Acidobacteriota)		Holophagae (Acidobacteriota)
			Acidimicrobiia (Actinobacteriota)		Coriobacteriia (Actinobacteriota)
			*Kapabacteria (Bacteroidota)		***Vampirivibrionia (Cyanobacteria)**
			Dehalococcoidia (Chloroflexi)		Desulfobulbia (Desulfobacterota)
			JG30-KF-CM66 (Chloroflexi)		*Desulfovibrionia (Desulfobacterota)
			*KD4_96 (Chloroflexi)		Syntrophia (Desulfobacterota)
			Lineage IIb (Elusimicrobiota)		Syntrophobacteria (Desulfobacterota)
			Candidate division WWE3 (Patescibacteria)		Syntrophobacteria (Desulfobacterota)
			Chlamydiae (Verrucomicrobiota)		Bacillia (Firmicutes)
					*Clostridia (Firmicutes)
					Desulfotomaculia (Firmicutes)
					Limnochordia (Firmicutes)
					Negativicutes (Firmicutes)
					Gemmatimonadetes (Gemmatimonadota)
					CPR2 (Patescibacteria)
					Planctomycetes (Planctomycetota)
					Spirochaetia (Spirochaetota)

	Rhizosphere	*WS2	*Blastocatellia (Acidobacteriota) Thermoleophilia (Actinobacteriota) Armatimonadia (Armatimonadota) *Kapabacteria (Bacteroidota) *KD4_96 (Chloroflexi) OLB14 (Chloroflexi) Saccharimonadia (Patescibacteria) Alphaproteobacteria (Proteobacteria)	*BD2-11 terrestrial group	***Vampirivibrionia (Cyanobacteria)** *Desulfovibrionia (Desulfobacterota) *Clostridia (Firmicutes)
Graphene	Bulk soil		Fimbriimonadia (Armatimonadota) bacteriap25 (Myxococcota) Leptospirae (Spirochaetota)		**Vampirivibrionia (Cyanobacteria)** Nitrospiria (Nitrospirota)
	Rhizosphere		Abditibacteria (Abditibacteriota) Subgroup 11 (Acidobacteriota) Polyangia (Myxococcota) Berkelbacteria (Patescibacteria)		Bdellovibrionia (Bdellovibrionota) Dabacteriia (Dadabacteria) **Planctomycetes (Planctomycetota)** Sumerlaeia (Sumerlaeota)

CNT enhanced microbial interactions in the tomato rhizosphere

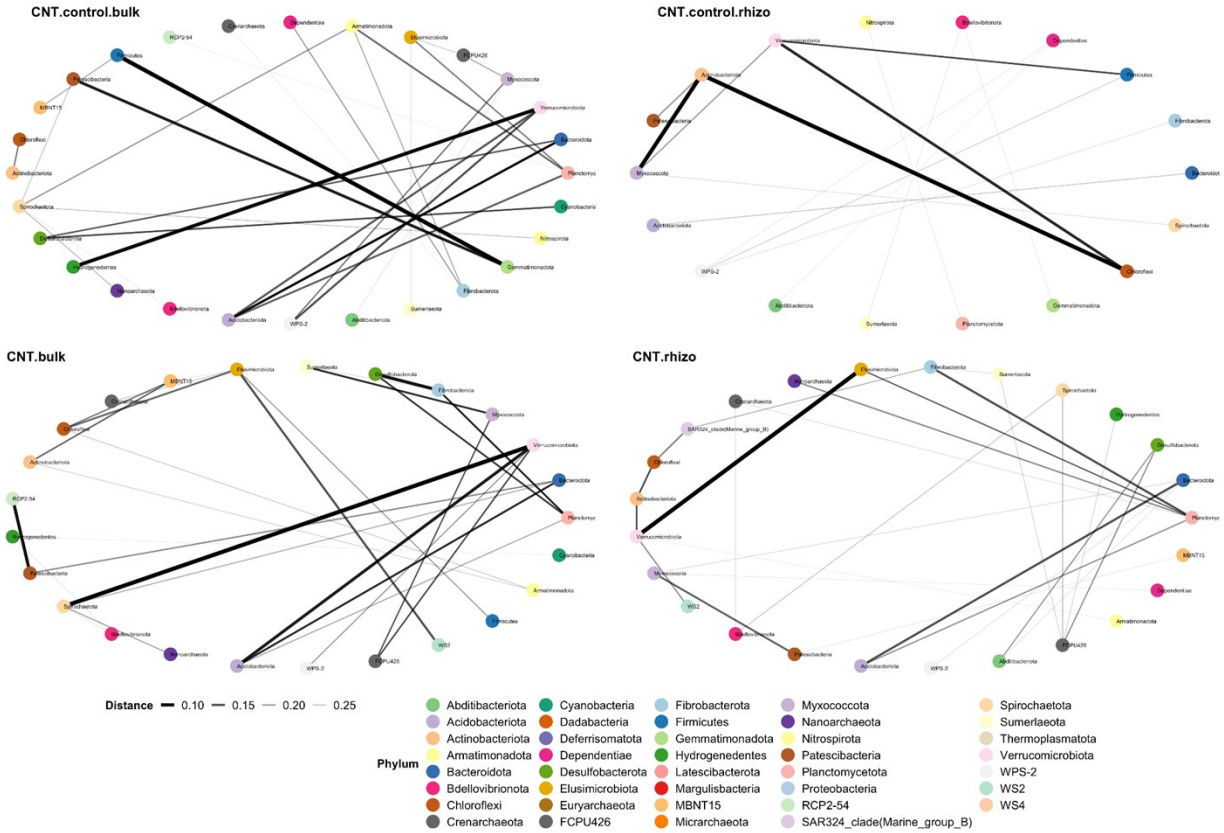

Figure S3. Effects of CNT on the class-level microbial network in the bulk soil and the tomato rhizosphere. Networks were calculated based on Bray-Curtis distance with a maximum distance of 0.3.

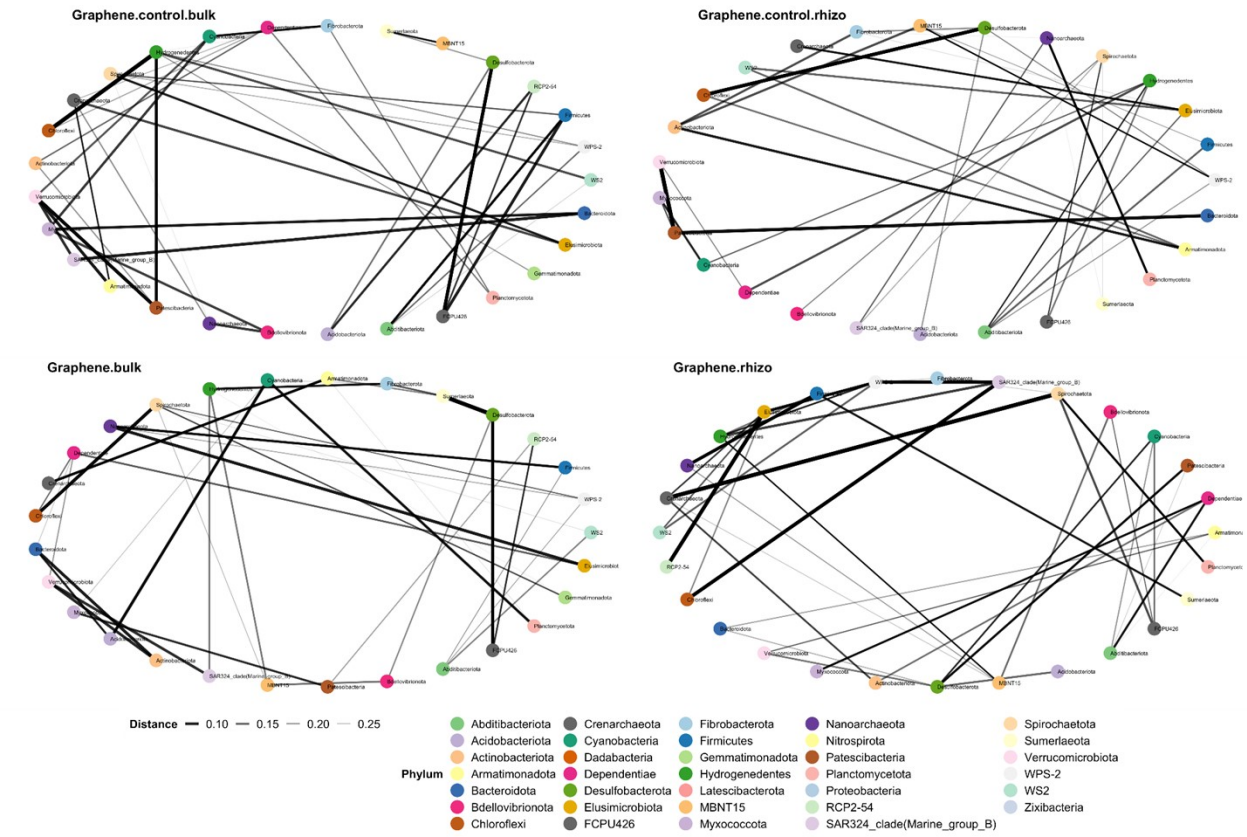

Figure S4. Effects of graphene on the class-level microbial network in the bulk soil and the tomato rhizosphere. Networks were calculated based on Bray-Curtis distance with a maximum distance of 0.3.

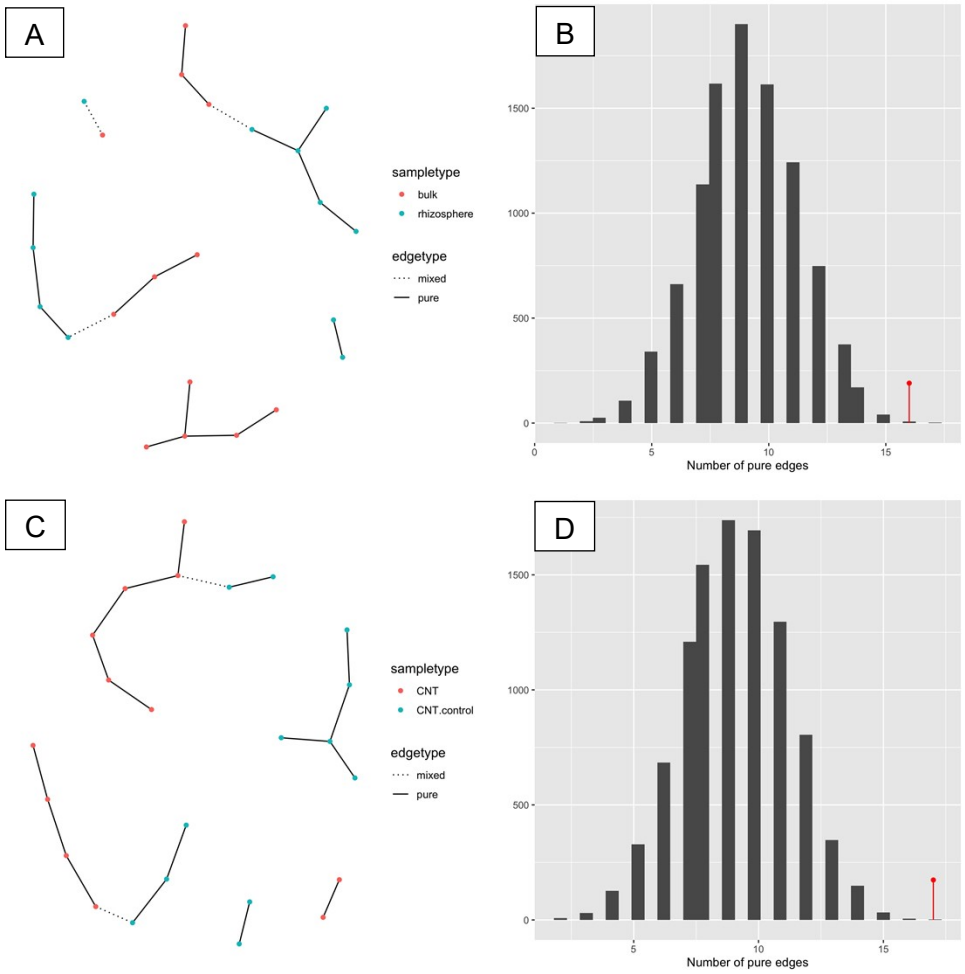

Figure S5. In the CNT experiment, soil zone (A, B) and treatment (C, D) are both significant factors shaping microbial network in the bulk soil and the tomato rhizosphere. (A, C) Nearest neighbor (NN) tree constructed on Bray-Curtis distance of agglomerated ASV abundance (to the phylum level) among treatment conditions (nodes). If from the same condition, nodes are connected by solid edges (pure), otherwise they are connected by dashed lines (mixed). Color denotes experimental condition. (B, D) Graph-based permutation test (n = 9999) on the nearest neighbor tree, $p < 0.002$ for both soil zone and treatment.

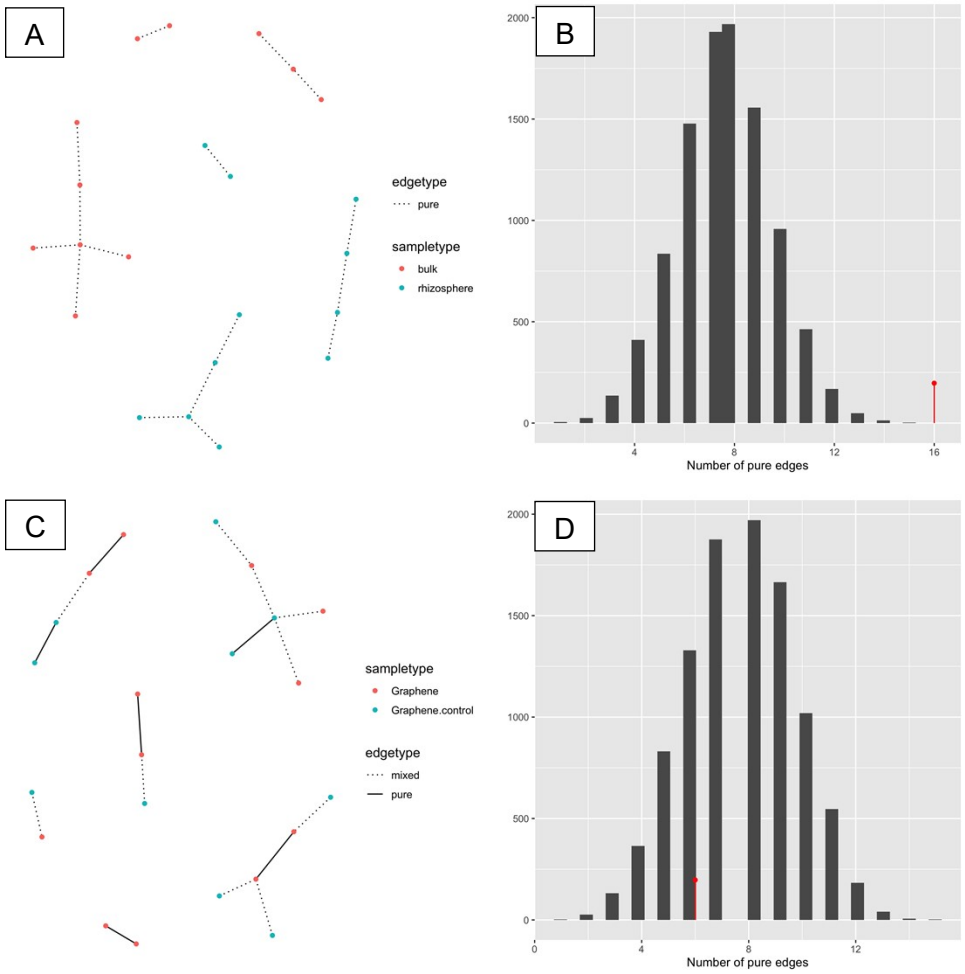

Figure S6. In the graphene experiment, soil zone (A, B) but not treatment (C, D) is a significant factor shaping microbial network in the bulk soil and the tomato rhizosphere. (A, C) Nearest neighbor (NN) tree constructed on Bray-Curtis distance of agglomerated ASV abundance (to the phylum level) among treatment conditions (nodes). If from the same condition, nodes are connected by solid edges (pure), otherwise they are connected by dashed lines (mixed). Color denotes experimental condition. (B, D) Graph-based permutation test (n = 9999) on the nearest neighbor tree, $p < 0.001$ for soil zone and $p = 0.864$ for treatment.

CNT-induced microbial functional changes

We used PICRUSt2 to infer microbial functions. The resulting NSTI values ranged from 0.135 to 0.258 for all the samples, suggesting a mid-range prediction accuracy typical for soil samples.[3] Rhizosphere samples showed smaller NSTI values than bulk soil samples ($p < 0.002$ in PERMANOVA after controlling treatment conditions), consistent with generally greater microbial diversity in bulk soil. Enriched pathways and modules were identified by DESeq2 in MicrobiomeAnalyst.[4,5] We chose DESeq2 because it uses shrinkage estimation for dispersions and fold changes for improved stability and interpretability of estimates, which enables a more quantitative analysis focused on the strength rather than the mere presence of differential presence.[4]

EcoPlate assay was used to compare community-level metabolism and substrate use patterns in bulk soils at the conclusion of the exposure experiment. After soil sample inoculation, we continuously monitored average well-color development (AWCD) for ~170 hours (Figure S8). AWCD values of the samples reached plateau after 7 days. Therefore, the final AWCD readings were used for calculation and cross-sample comparison. Soil basal respiration was also estimated for bulk soil samples (Figure S9). CNT treatment significantly increased basal respiration in bulk soils ($p < 0.03$ in ANOVA followed by Tukey's HSD). Graphene did not have significant effect on basal soil respiration in bulk soils.

Table S3. CNT-induced changes in microbial functional pathways in bulk soil and the tomato rhizosphere. Functional inference was conducted using PICRUSt2.

Soil zone	Pathway	Total	Expected	Hits	*P*-value	FDR	KO Hits
Bulk soil	Nitrogen metabolism	49	2.060	10	0.0000248	0.00392	K03385 K02588 K15876 K05601 K02586 K02591 K15371 K00376 K01915 K01674
	Amino sugar and nucleotide sugar metabolism	126	5.300	13	0.00205	0.162	K02795 K02796 K02794 K00844 K02564 K12454 K00849 K01209 K01809 K00963 K10012 K16011 K02377
	Fructose and mannose metabolism	88	3.700	10	0.00336	0.177	K02795 K02796 K02794 K00844 K07046 K02770 K01809 K00895 K16011 K02377

Bulk soil	Chloroalkane and chloroalkene degradation	28	1.180	5	0.00548	0.216	K02588 K02586 K02591 K00121 K00114
	Pyruvate metabolism	86	3.620	9	0.00917	0.290	K00625 K00626 K01067 K00656 K01571 K01960 K01596 K01573 K01069
	Ascorbate and aldarate metabolism	38	1.600	5	0.020	0.484	K02822 K13875 K00469 K13876 K03077
	Fatty acid degradation	39	1.640	5	0.0222	0.484	K00626 K06445 K00121 K01692 K00249
	Carbon fixation pathways in prokaryotes	101	4.250	9	0.0245	0.484	K00625 K00626 K00176 K00177 K00198 K15022 K01960 K00196 K00242
	Sulfur metabolism	74	3.110	7	0.0341	0.516	K01011 K00956 K08354 K08352 K00380 K00955 K01082

Bulk soil	Fatty acid metabolism	60	2.520	6	0.0384	0.516	K00626 K06445 K16363 K01692 K00249 K01716
	Porphyrin and chlorophyll metabolism	76	3.200	7	0.0387	0.516	K04040 K03428 K04037 K04038 K04039 K10960 K03403
	Methane metabolism	147	6.180	11	0.0427	0.516	K00625 K12234 K03388 K11212 K00121 K00198 K15022 K00196 K03390 K11261 K02203
	Biosynthesis of amino acids	223	9.380	15	0.0446	0.516	K01914 K11358 K05825 K05822 K05823 K13853 K17462 K14155 K01960 K01243 K01915 K02502 K03785 K14682 K02203
Rhizosphere	Toluene degradation	38	1.63	15	9.70E-12	1.53E-09	K16242

Rhizosphere	Toluene degradation						K16243 K16244 K16245 K16246 K16249 K00141 K05797 K07540 K07543 K07545 K07547 K07548 K07549 K07550
	Degradation of aromatic compounds	171	7.35	26	5.95E-09	4.70E-07	K04072 K16242 K16243 K16244 K16245 K16246 K07537 K16249 K00141 K10216 K05712 K05783 K04108 K07540 K18074 K18076 K07536 K16050 K07543 K07545 K07547 K07548 K07549 K07550 K16049 K05550

Rhizosphere	Benzoate degradation	82	3.53	17	3.22E-08	1.69E-06	K04098 K16242 K16243 K16244 K16245 K16246 K07537 K16249 K04110 K10216 K05783 K10221 K04108 K01615 K07536 K05550 K04100
	Steroid degradation	9	0.387	4	0.000348	0.0115	K16050 K05898 K16049 K15982
	Chlorocyclohexane and chlorobenzene degradation	33	1.42	7	0.000389	0.0115	K04098 K16242 K16243 K16244 K16245 K16246 K16249
	Methane metabolism	147	6.32	16	0.000438	0.0115	K00196 K01007 K03389 K05979 K03390 K11781 K11780 K16792 K00148 K11212 K12234 K00198

Rhizosphere							K15022 K03388 K18277 K03841
	Phenylalanine metabolism	76	3.27	10	0.0013	0.0294	K01912 K10775 K11358 K05712 K02614 K02610 K02611 K02612 K02609 K02613
	Aminobenzoate degradation	35	1.51	5	0.0157	0.309	K00141 K04110 K10221 K04108 K04100
	Ubiquinone and other terpenoid-quinone biosynthesis	50	2.15	6	0.0189	0.332	K05928 K03182 K09833 K09834 K18534 K12073
	Carotenoid biosynthesis	28	1.2	4	0.030	0.474	K09835 K02293 K14605 K14606
	Xylene degradation	32	1.38	4	0.0462	0.659	K00141 K10216 K05783 K05550

Table S4. CNT-induced changes in microbial functional modules in bulk soil and the tomato rhizosphere. Functional inference was conducted using PICRUSt2.

Soil zone	Module	Total	Expected	Hits	*P*-value	FDR	KO Hits
Bulk soil	Nitrogen fixation, nitrogen => ammonia	4	0.170	3	0.000282	0.067	K02588 K02586 K02591
	Assimilatory sulfate reduction, sulfate => H_2S	10	0.424	3	0.00704	0.830	K00956 K00380 K00955
	Methanogenesis, acetate => methane	13	0.552	3	0.0153	0.944	K00625 K03388 K03390
	F_{420} biosynthesis	6	0.255	2	0.0238	0.944	K12234 K11212
	Incomplete reductive citrate cycle, acetyl-CoA => oxoglutarate	17	0.721	3	0.0323	0.944	K00176 K00177 K01960
	Nucleotide sugar biosynthesis, glucose => UDP-glucose	7	0.297	2	0.0324	0.944	K00844 K00963
	Cysteine biosynthesis, methionine => cysteine	7	0.297	2	0.0324	0.944	K17462 K01243
	Ascorbate degradation, ascorbate => D-xylulose-5P	7	0.297	2	0.0324	0.944	K02822 K03077
	Methanogenesis, CO2 => methane	19	0.806	3	0.0433	0.944	K03388 K03390 K11261
	beta-Oxidation	19	0.806	3	0.0433	0.944	K06445 K01692 K00249
Rhizosphere	Benzene degradation, benzene => catechol	6	0.303	6	1.34E-08	2.42E-06	K16242 K16243 K16244 K16245 K16246 K16249
	Toluene degradation, anaerobic, toluene => benzyl-CoA	9	0.454	7	2.05E-08	2.42E-06	K07540 K07543 K07545

							K07547 K07548 K07549 K07550
	Tocopherol biosynthesis	5	0.252	4	2.87E-05	0.00226	K05928 K09833 K09834 K18534
	F_{420} biosynthesis	6	0.303	4	8.28E-05	0.00489	K11781 K11780 K11212 K12234
	Methanogenesis, methanol => methane	9	0.454	3	0.00831	0.392	K03389 K03390 K03388
	Benzoate degradation, benzoate => catechol / methylbenzoate => methylcatechol	4	0.202	2	0.0141	0.476	K05783 K05550
	Terephthalate degradation, terephthalate => 3,4-dihydroxybenzoate	4	0.202	2	0.0141	0.476	K18074 K18076
	Methanogenesis, acetate => methane	13	0.656	3	0.0245	0.641	K03389 K03390 K03388
	Methanogenesis, methylamine/dimethylamine/trimethylamine => methane	13	0.656	3	0.0245	0.641	K03389 K03390 K03388
	beta-Carotene biosynthesis, GGAP => beta-carotene	6	0.303	2	0.033	0.779	K09835 K02293
	Reductive pentose phosphate cycle, ribulose-5P => glyceraldehyde-3P	7	0.353	2	0.0447	0.96	K00150 K01602

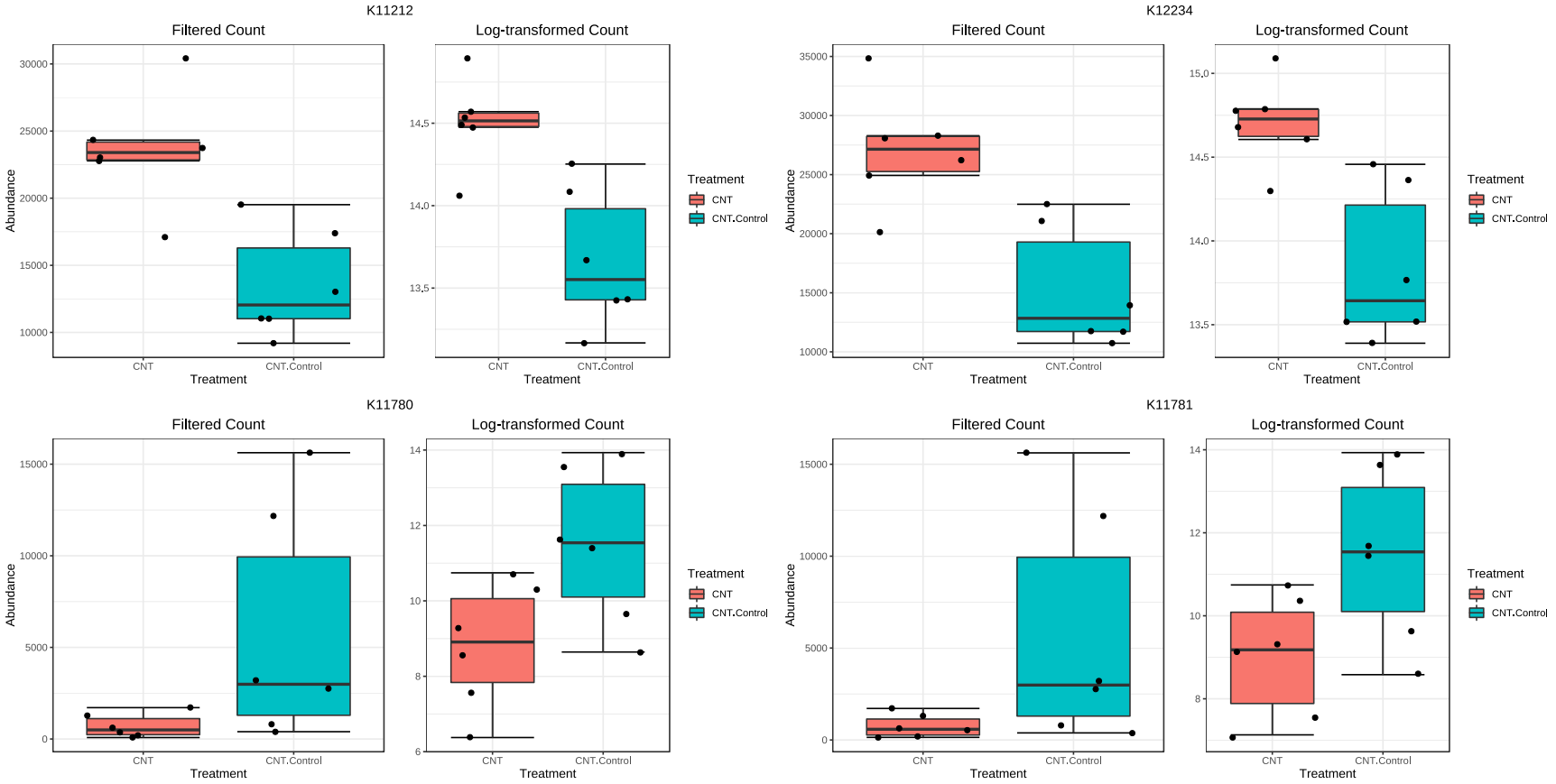

Figure S7. CNT effects on F_{420} biosynthesis in the tomato rhizosphere. K11212: *cofD* gene encoding 2-phospho-L-lactate transferase; K12234: *cofE* gene encoding coenzyme F420:L-glutamate ligase; K11780: *cofG* encoding 7,8-didemethyl-8-hydroxy-5-deazariboflavin synthase; K11781: *cofH* gene encoding 5-amino-6-(D-ribitylamino)uracil-L-tyrosine 4-hydroxyphenyl transferase.[6]

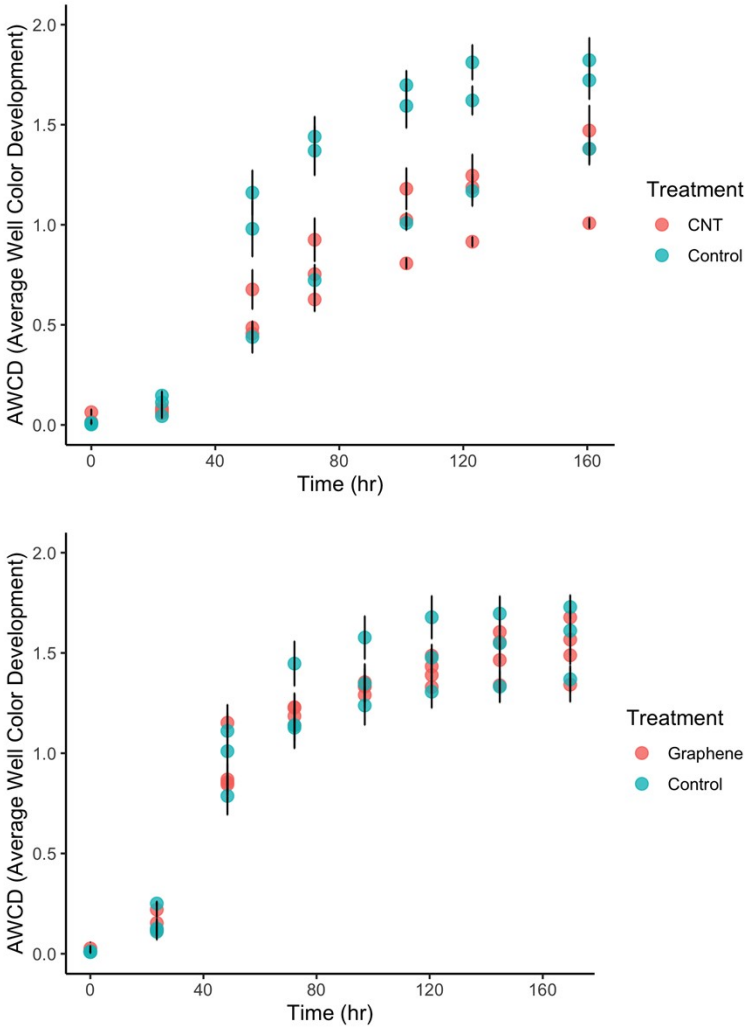

Figure S8. AWCD of bulk soils harvested by the end of the CNT or graphene experiment. Data points represent average across 3 technical replicates and 3-4 biological replicates; bars represent standard deviation.

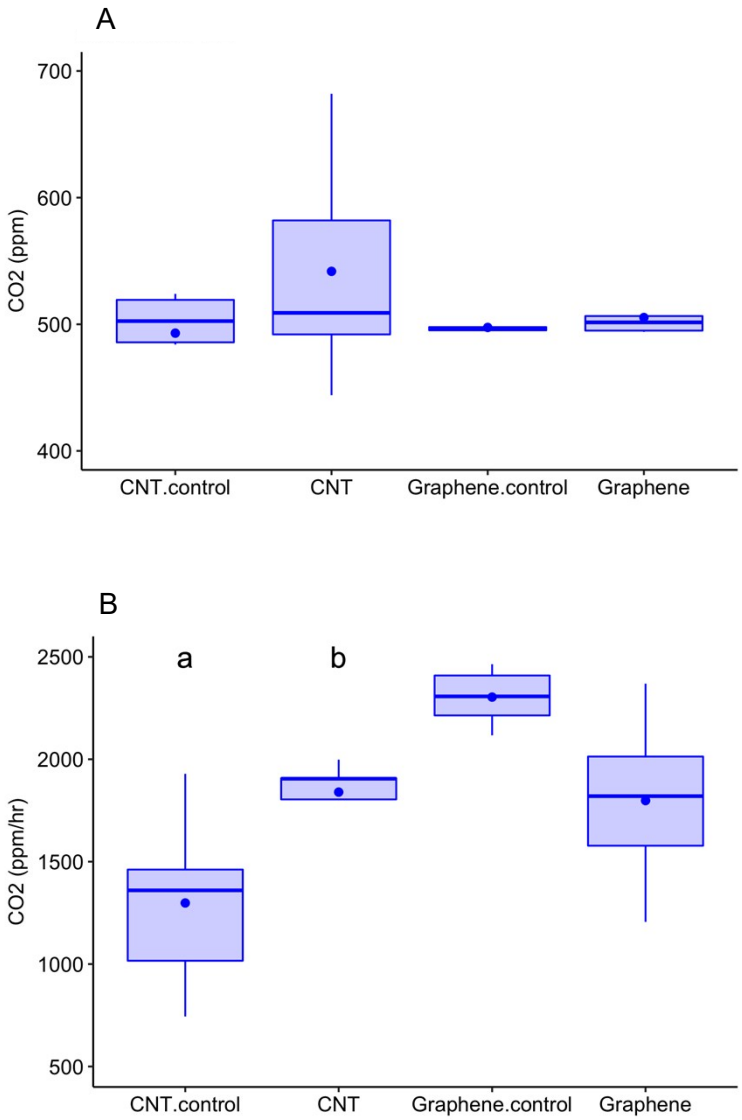

Figure S9. (A) Ambient CO_2 measured at the time of soil respiration assessment. No significant difference was observed among measurements. (B) Soil basal respiration rate (hourly CO_2 generation) in the treated and untreated soils. Letters indicate statistical significance ($p < 0.03$ in ANOVA followed by Tukey's HSD).

References

1. S. R. Olsen, Estimation of available phosphorus in soils by extraction with sodium bicarbonate (No. 939), US Department of Agriculture, 1954.

2. L. E. Allison and C. D. Moodie, Carbonate. Methods of Soil Analysis: Part 2 Chemical and Microbiological Properties, 1965, **9**, 1379-1396.

3. G. M. Douglas, V. J. Maffei, J. R. Zaneveld, S. N. Yurgel, J. R. Brown, C. M. Taylor, C. Huttenhower and M. G. Langille, PICRUSt2 for prediction of metagenome functions, *Nat. Biotechnol.*, 2020, **38**, 685-688.

4. M. I. Love, W. Huber and S. Anders, Moderated estimation of fold change and dispersion for RNA-seq data with DESeq2, *Genome Biol.*, 2014, **15**, 1-21.

5. J. Chong, P. Liu, G. Zhou and J. Xia, Using MicrobiomeAnalyst for comprehensive statistical, functional, and meta-analysis of microbiome data, *Nat. Protoc.*, 2020, **15**, 799-821.

6. R. Grinter and C. Greening, Cofactor F420: An expanded view of its distribution, biosynthesis and roles in bacteria and archaea, *FEMS Microbiol. Rev.*, 2021, **45**, fuab021.